Induced noncollinear magnetic order of Nd^{3+} in $NdNiO_3$ observed by resonant soft x-ray diffraction

V. Scagnoli*
European Synchrotron Radiation Facility, Boîte Postale 220, 38043 Grenoble, Cedex 9, France

U. Staub, Y. Bodenthin, and M. García-Fernández
Paul Scherrer Institut, Villigen PSI 5232, Switzerland

A. M. Mulders
Paul Scherrer Institut, Villigen PSI 5232, Switzerland;
Department of Imaging and Applied Physics, Curtin University of Technology, Perth, Western Australia 6845, Australia;
and The Bragg Institute, Australian Nuclear Science and Technology Organization, Lucas Heights, New South Wales 2234, Australia

G. I. Meijer and G. Hammerl
IBM Research, Zurich Research Laboratory, 8803 Rüschlikon, Switzerland
(Received 29 October 2007; published 27 March 2008)

Soft x-ray resonant magnetic diffraction at the Nd *M* edges was performed on a $NdNiO_3$ epitaxial film to investigate the magnetic ordering of the Nd ions below the metal-insulator transition. A noncollinear magnetic structure induced by the Ni magnetic moments best describes the azimuthal angle dependency of the $(1/2,0,1/2)$ reflection. This confirms the Ni spin structure observed with soft x-ray diffraction experiments performed at the Ni *L* edge, providing further evidence of charge disproportionation without orbital order below the metal-insulator transition in $NdNiO_3$.

DOI: 10.1103/PhysRevB.77.115138 PACS number(s): 78.70.Ck, 71.30.+h

I. INTRODUCTION

In recent years, investigations have been made of charge localization in compounds which show an abrupt metal-to-insulator (MI) transition. Of particular interest is the interaction between the charge, orbital, and magnetic degrees of freedom. To understand the MI phase transition, the choice of model compound is paramount in order to reduce the number of degrees of freedom. The nickelate family $RNiO_3$ (where *R* stands for a rare-earth or Y ion) represents a promising candidate, due to its simple stoichiometry (no chemical doping is needed to obtain a metallic phase) and the relatively simple orthorhombic lattice symmetry, with Ni ions at high symmetry positions.[1]

$RNiO_3$ compounds exhibit a MI transition which depends on the magnitude of the rare-earth ionic radius. From the unusual magnetic structure characterized by a $(1/2,0,1/2)$ wave vector, an up-up-down-down stacking of Ni magnetic moments was proposed, implying an orbital ordering of the Ni^{3+} e_{g1} electrons.[2,3] For the heavier rare-earth compounds, charge order, also called charge disproportionation in the case of fractional charge quantities, was found by bond valence sum considerations.[4] Resonant x-ray diffraction at the *K* edge demonstrated that charge ordering also occurs for $NdNiO_3$.[5,6] Recent calculations and pressure-dependent experiments on $LuNiO_3$ support the lifting of orbital degeneracy through charge ordering as an alternative to Jahn-Teller distortion.[7] This mechanism appears to occur also in other materials such as ferrates.[8]

A neutron powder diffraction study of $HoNiO_3$ is equally well described with a collinear up-up-down-down magnetic structure as with a noncollinear magnetic structure of the Ni ions.[9] Low temperature specific heat measurements of $NdNiO_3$ question[10] the Nd magnetic structure suggested by neutron diffraction.[2,3] Recent resonant soft x-ray diffraction data on $NdNiO_3$ indicate that the Ni magnetic structure is noncollinear,[11] consistent with the charge ordering but inconsistent with orbital order. These results have a strong impact on the properties of the material as an up-up-down-down magnetic structure can induce ferroelectricity.[12] In addition, the study of the magnetic degree of freedom in this particular system is interesting because the MI transition coincides with the establishment of an antiferromagnetic structure ($T_{MI}=T_N$). This coincidence is unique to Nd and Pr in the $RNiO_3$ series: for the heavier rare-earth ions $T_{MI}>T_N$.

In this work, we present results of a soft x-ray resonant diffraction study of the Nd magnetic moments. The Nd magnetic structure results from Nd-Ni exchange. Therefore, a careful study of the magnetic structure of the Nd ions will provide an independent means to discriminate between the proposed magnetic structures of the Ni ions.

The method of choice to determine magnetic structure is neutron diffraction, but crystalline samples of sufficient size are not available. X-ray diffraction is then the best option, in particular, using resonant scattering at the magnetic ion absorption edges.[13] In this technique, an incident photon promotes a core electron to an excited intermediate state that subsequently decays to the initial state, emitting a scattered photon. This resonance process enhances the magnetic signal and the contribution of the resonant ions is identified separately from other atomic species in the structure.

Consequently resonant x-ray diffraction, recently developed in the soft x-ray regime,[14–17] represents a very sensitive tool to investigate condensed matter. The possibility to vary

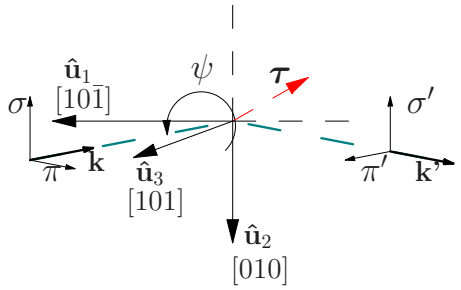

FIG. 1. (Color online) Resonant soft x-ray diffraction geometry at the RESOXS end station. The polarization of the incident x rays is either σ or π. $\hat{u}$ indicates the experimental coordinate system and ψ the azimuthal angle. **k** and **k′** are the wave vectors of the incident and diffracted x rays respectively, and τ is the scattering vector.

the energy of the incident photons gives the flexibility to probe different electronic shells, either of the same ionic species or of different ions. It is particularly interesting to probe the valence shell which is responsible for the magnetism.

In order to fully characterize the magnetic structure of $NdNiO_3$, resonant soft x-ray experiments were performed at the Nd M edges. Detailed characterization of the magnetic reflection through its energy and azimuthal angle (rotation of the sample about the diffraction wave vector) dependences strongly constrains the allowed magnetic structures.

II. EXPERIMENT

A high-quality epitaxial film of $NdNiO_3$ was grown on a [101] oriented $NdGaO_3$ substrate (*Pbnm*) by pulsed laser deposition. Polycrystalline $NdNiO_3$, synthesized as in Ref. 18, was used as the ablation target. The films were deposited in a 0.3 mbar oxygen atmosphere at $T=740$ °C. After deposition, the sample was cooled slowly in a controlled oxygen atmosphere of 1 bar. The energy of the KrF excimer laser was 800 mJ with 5 Hz repetition rate. The thickness of the resulting $NdNiO_3$ film was approximately 500 Å. The resistivity of the film was measured with conventional four-probe technique; it shows a first-order metal-insulator transition at approximately $T=200$ and 180 K,[19] upon heating and cooling, respectively. T_{MI} is lower than in polycrystalline $NdNiO_3$, probably because of epitaxial strain. No impurity phases were detected with Cu $K\alpha$ x-ray diffraction. The full width at half maximum of the rocking curve of the films was 0.14°. Polarized soft x-ray diffraction experiments were performed at the SIM beamline of the Swiss Light Source at the Paul Scherrer Institut using the RESOXS end station.[20] Measurements were performed at the Nd $M_{4,5}$ edges between 30 and 300 K using a continuous helium-flow cryostat. Azimuthal scans were obtained by sample rotation with an accuracy of approximately 5°. The linear polarization of the incoming beam was chosen either horizontal (π) or vertical (σ) with respect to the diffraction plane. Figure 1 shows the experimental geometry. The azimuthal angle $\psi=0°$ corresponds to the [010] crystallographic direction perpendicular to the diffraction plane. Diffracted intensities were recorded with an AXUV-100 photodiode from International Radiation

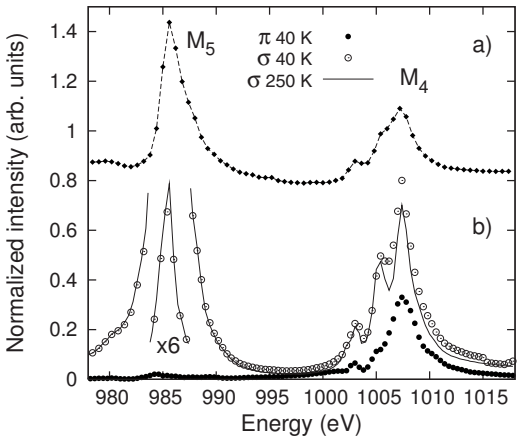

FIG. 2. (a) Fluorescence at the Nd M edges, recorded with the CCD camera. (b) Intensity of the (1/2,0,1/2) reflection recorded with the CCD camera, at the Nd M edges at $T=40$ K and $\psi=0°$ for π (filled circles) and σ (open circles) incident radiation. A spectrum recorded at 250 K with σ incident radiation (continuous line) is also shown.

Detectors and with an in-vacuum charge-coupled device (CCD) camera from Roper Scientific. The latter shows improved signal to noise ratio and was used to record selected energy dependent intensities. The recorded CCD images were corrected for background (recorded without incoming radiation), integrated along the camera height and fitted with a Lorentzian and a linear background, in order to extract the integrated intensity and background due to the sample, respectively. In fact, this background is due to the fluorescence originating from the sample and provides a means of simultaneously recording the absorption. Polarization analysis was performed in the soft x-ray regime,[11,21] but the observed signal at the Nd M_4 edge was too weak to resolve.

III. RESULTS

The energy dependence of the integrated intensity of the (1/2,0,1/2) reflection at $\psi=0°$ recorded with the CCD camera for both π and σ incident polarizations is shown in Fig. 2(b). The intensity for σ incident radiation is dominated by the reflectivity, as a comparison between the spectra above (250 K) and below (40 K) the MI transition temperature illustrates. An additional signal, arising from magnetic diffraction, is present at the Nd M_4 edge at 40 K. However, it is weak compared to the reflectivity.

Because the diffraction angle is close to 45°, the reflectivity for π incident radiation is strongly suppressed. Therefore, the sample acts as a polarizer, and the diffracted intensity recorded with π incident radiation is due mainly to the (1/2,0,1/2) superlattice reflection. The strong resonance at the Nd M_4 edge, compared to M_5, is a typical feature of magnetic resonant diffraction, as expected for an ion with less than half filling in the valence shell, e.g., USb.[22] The energy dependence recorded with the photodiode for $\psi=90°$ shows a similar energy profile, but with a reduced intensity (not shown). Note that the Nd M_4 edge is contiguous with the Ni L_1 edge; they are separated by approximately

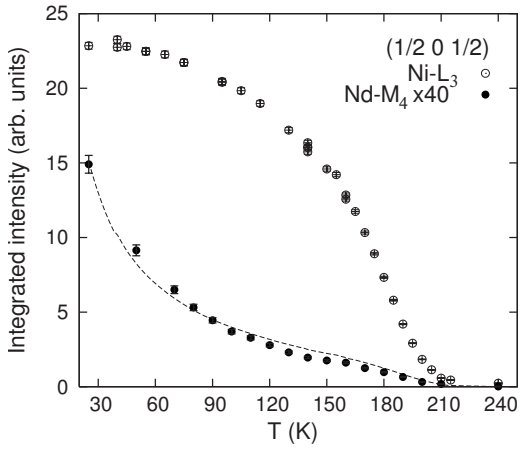

FIG. 3. Temperature dependence of the $(1/2,0,1/2)$ diffracted intensity at the Nd M_4 edge (filled circles) compared to that recorded at Ni L_3 edge (open circles) (Ref. 11). The dotted line corresponds to the calculated intensity originating from the Nd magnetic moments that are induced by the Ni magnetic order, as explained in the text.

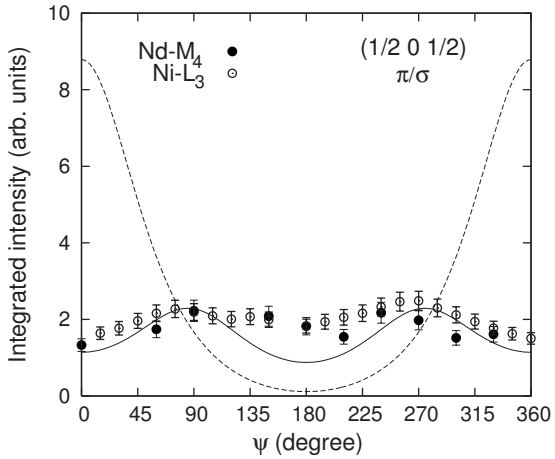

FIG. 4. Azimuthal angle dependence of the $(1/2,0,1/2)$ reflection at the Nd M_4 edge recorded at $T=35$ K compared to the azimuthal angle dependence recorded at the Ni L edge. The solid and dotted lines correspond to the noncollinear and up-up-down-down magnetic structures, respectively.

5 eV. This electronic transition involves an s-type shell which is only very weakly sensitive to magnetism, as evidenced by studies performed at the Ni K edge.[6] Indeed this transition probes only the orbital moment of the p shell, which is expected to be very small.

Figure 3 shows the temperature dependence of the $(1/2,0,1/2)$ reflection at the Nd M_4 edge, recorded with π incident radiation. The temperature dependence of the same reflection recorded at the Ni L edge is shown for comparison, reproduced from Ref. 11. The temperature dependence is very different in the two cases: At the Ni L edge, the increase in intensity below T_{MI} follows the behavior of a typical order parameter squared, as expected for a second order magnetic phase transition. At the Nd M edge, however, a gradual increase in intensity is observed below T_{MI}, and a steep increase occurs below ~70 K. This indicates that the Nd magnetic order is induced by the Ni moments that order spontaneously in the insulating phase. A quantitative description will be presented in the following section. In addition, $\theta/2\theta$ scans were recorded at the Nd M_4 edge (1008 eV), with both incident π and σ radiation for various orientations of ψ. This procedure ensures that the total reflectivity, especially strong with σ incident radiation, only appears as part of the background. In the soft x-ray energy range, the Ewald sphere is often limited to superlattice reflections and in our case excludes a normalization with a Bragg reflection. Therefore we consider the π/σ ratio, to prevent systematic errors (e.g., from sample size and beam shape effect) that are not easy to correct for. Figure 4 shows π/σ together with the same result collected at the Ni L_3 edge.[11] The azimuthal angle dependence at the Nd M_4 edge has the same ratio and periodicity as the one at the Ni L edges. A comparison with calculations will be given in the following section.

IV. DISCUSSION

Interpretation of resonant diffraction data can be controversial, in particular, when charge, magnetic, and orbital scattering can occur at the same position in reciprocal space. Following Ref. 23, the resonant atomic scattering amplitude in the vicinity of an absorption edge is given by

$$f(\mathbf{k},\mathbf{k}',E) = f_0(\mathbf{k}-\mathbf{k}') + f'(\mathbf{k},\mathbf{k}',E) + if''(\mathbf{k},\mathbf{k}',E) + f^{mag}(\mathbf{k},\mathbf{k}',E), \quad (1)$$

where f_0 is the Thomson charge scattering amplitude and f^{mag} the resonant magnetic scattering amplitude. $\mathbf{k},\mathbf{k}'$ and $E=\hbar\omega$ are the incident and outgoing wave vectors and photon energy, respectively. f' and f'' are energy dispersive terms, which become significant close to the absorption edges.

In the proceeding, we discussed the origin of the forbidden $(1/2,0,1/2)$ reflection. Charge diffraction is unlikely, as it was not observed at the Ni K edge at this particular point of reciprocal space.[6] Moreover, charge scattering with incident π radiation is strongly suppressed [by the factor $\cos(2\theta)$] for an incident angle close to 45°, as in the present case. Diffraction originating from the anisotropy of the susceptibility tensor, so called Templeton and Templeton scattering,[24] typically produces significantly different intensities for σ and π incident radiation, since contributions from $\sigma-\sigma'$ and $\pi-\pi'$ are dissimilar. The diffracted intensity for this scattering shows a stronger signal for σ incident radiation, since the $\pi-\pi'$ component decreases with increasing Bragg angle.[25] On the other hand, diffraction due to magnetic moments does not show intensity for $\sigma-\sigma'$. In addition, all the magnetic models considered here (see the Appendix) predict no intensity contribution from the $\pi-\pi'$ channel for $\psi=0°$. A comparable signal, arising from the rotated light ($\sigma-\pi'$ or $\pi-\sigma'$), would then be expected, regardless of the incoming polarization.

Therefore, the $(1/2,0,1/2)$ reflection is likely of magnetic origin, and we analyze the temperature dependence and the azimuthal angle dependence accordingly. In this case, the diffracted intensity is proportional to the square of the expectation value of the magnetic Nd moments. The temperature

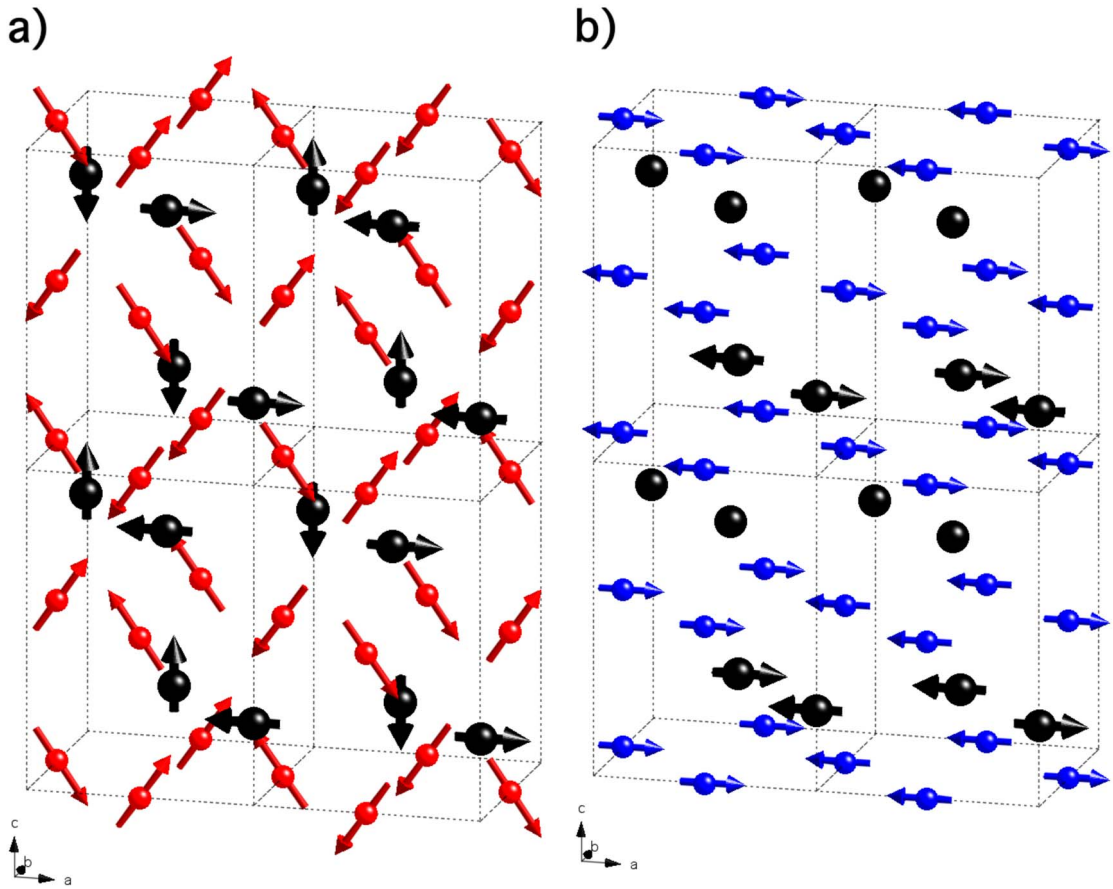

FIG. 5. (Color online) Two magnetic structures that have been proposed for $NdNiO_3$: (a) The noncollinear magnetic structure (Ref. 11); (b) the up-up-down-down magnetic structure (Ref. 2). Nd and Ni ions are indicated by large (black) and small (red or blue) spheres, respectively. Magnetic moment directions are indicated with arrows.

dependence suggests that the Nd magnetic moments are induced, and that the effective magnetic field acting on the Nd ions is generated by the ordered magnetic moments of the Ni ions. In this case, the magnetization **M** of the Nd $4f$ electrons is parallel to the magnetic field **H** generated by the Ni moments, and its magnitude is given by[26]

$$M = \frac{N}{V} g \mu_B J B_J \left(\frac{g \mu_B J H}{k_B T} \right), \tag{2}$$

where N is the number of Nd ions in the volume V, g is the Lande actor, μ_B is the Bohr magneton, T is the temperature, and k_B is the Boltzmann constant. $B_J(x)$ is the Brillouin function, and J is the total angular momentum of the Nd $4f$ shell.

The magnitude of **H** is proportional to the Ni moment and is proportional to the square root of the intensity of the magnetic reflection at the Ni L_3 edge. The Nd^{3+} ions are expected to be in their ground multiplet $^4I_{9/2}$.

Figure 3 shows the result of this model, fitted to the experimental data. The agreement confirms that the Nd magnetic moments are indeed induced by the magnetic moments of the Ni ions. We note that one parameter, an overall scaling factor, was varied in this fit. This confirms the magnetic origin of the forbidden $(1/2,0,1/2)$ reflection. Induced magnetic order was also observed with resonant x-ray diffraction at the Nd L edges in Nd_2CuO_4.[27] Figure 4 shows that the π/σ ratio has the same periodicity and magnitude as a function of azimuthal angle as for the case of Ni L edges. To test the magnetic structures proposed in Refs. 2 and 11 (see Fig. 5), the so-called up-up-down-down and noncollinear structures, respectively, we calculate the azimuthal dependences of the $(1/2,0,1/2)$ reflection using the formalism of Hill and McMorrow.[28]

The up-up-down-down model leads to two different environments for the Nd ions. The so-called B^0 Nd layers, with four up and four down Ni neighbors, and the so-called $B^{\pm}$ Nd layers, with six up and two down Ni neighbors. The ordering of Ni magnetic moments induces a Nd magnetic moment in the $B^{\pm}$ layer while the Nd ions in the B^0 layers remain paramagnetic. The noncollinear structure leads to Nd magnetic moments that can be divided into two groups. In the first group, the Nd magnetic moments are parallel to the a axis, while in the second group, they are parallel to the c axis.

In the Appendix , we calculate the polarization dependent diffracted intensity of the $(1/2,0,1/2)$ reflection due to the Nd magnetic moments, for both magnetic structures. The π/σ ratios obtained are shown in Fig. 4 as function of azimuthal angle. The up-up-down-down structure does not describe the experimental data, while the noncollinear structure

is in good agreement with the measurements. This interpretation is also supported by specific heat measurements,[10] which find that *all* the Nd ions experience the Ni-Nd exchange field. Therefore the magnetic order of the Nd magnetic moments is consistent with the Ni magnetic structure obtained by resonant x-ray diffraction (RXD) at the Ni L edges.[11] No orbital ordering (often associated with Jahn-Teller distortions) occurs at the phase transition, in agreement with Ref. 7.

V. CONCLUSIONS

Soft x-ray resonant diffraction at the Nd M edges has been used to determine the magnetic structure of the Nd ions in $NdNiO_3$. Energy, temperature, and azimuthal angle dependences were used to infer the magnetic origin of the diffracted $(1/2,0,1/2)$ intensity. The results are in good agreement with a noncollinear structure of the Nd magnetic moments, induced by the noncollinear Ni magnetic moments. This further supports the absence of orbital order in $NdNiO_3$. This paper demonstrates that RXD can be a useful tool for determining magnetic structures when neutron diffraction is inconclusive or infeasible.

ACKNOWLEDGMENTS

We thank the beamline staff of X11MA for its excellent support. This work was supported by the Swiss National Science Foundation and performed at SLS of the Paul Scherrer Institut, Villigen PSI, Switzerland.

APPENDIX

The azimuthal angle and polarization dependence of the magnetic reflection are calculated in three steps. First, the structure factor for the magnetic unit cell is calculated considering the Nd ions only. Second the orientation of the magnetic Nd moments is calculated as a function of the azimuthal angle. Finally, the polarization dependence of the incident and diffracted x rays is evaluated, following the formalism of Ref. 28.

For both magnetic structures, the Nd magnetic moments are in the a,c plane, and the magnetic moment direction is described universally by the angle α, resulting in the vector $\mathbf{m}=[\cos(\alpha),0,\sin(\alpha)]$. α is zero when the magnetic moment is oriented parallel to the a axis. A rotation $R(\beta)$ about the u_2 axis aligns the sample along the wave vector $\tau=(1/2,0,1/2)$; in this case $\beta=125.89°$. $R(\psi)$ represents the azimuthal angle rotation about τ as follows:

$$R(\beta)=\begin{pmatrix}\cos(\beta) & 0 & \sin(\beta)\\ 0 & 1 & 0\\ -\sin(\beta) & 0 & \cos(\beta)\end{pmatrix}, \tag{A1}$$

$$R(\psi)=\begin{pmatrix}1 & 0 & 0\\ 0 & \cos(\phi) & -\sin(\psi)\\ 0 & \sin(\psi) & \cos(\psi)\end{pmatrix}. \tag{A2}$$

This results in the vector $\mathbf{z}=R(\psi)R(\beta)\mathbf{m}$ as follows:

$$\mathbf{z}=\begin{pmatrix}\cos(\psi)[\cos(\beta)\cos(\alpha)+\sin(\beta)\sin(\alpha)]\\ \sin(\psi)[\cos(\beta)\cos(\alpha)+\sin(\beta)\sin(\alpha)]\\ -\sin(\beta)\cos(\alpha)+\cos(\beta)\sin(\alpha)\end{pmatrix}.$$

The polarization dependence is obtained from Ref. 28 and is given by

$$M(\theta)=\begin{pmatrix}0 & z_3\sin\theta+z_1\cos\theta\\ z_3\sin\theta-z_1\cos\theta & -z_2\sin(2\theta)\end{pmatrix}.$$

$M(\theta)$ represents the magnetic diffraction, in the case of an electric dipole transition (E1), and its components are characterized by σ,π incident and σ',π' diffracted radiation. We calculate the diffracted intensity of each component as a function of the azimuthal angle for the two magnetic structures under consideration.

1. Up-up-down-down magnetic structure

The Nd magnetic moments are parallel to the a axis [see Fig. 5(b)], and α is equal to 0. The magnetic structure factor is imaginary, and $\mathbf{z}=[\cos(\psi)\cos(\beta),\sin(\psi)\cos(\beta),-\sin(\beta)]$. Substituting $\mathbf{z}$ in $M(\theta)$ and calculating the intensity of the diffracted signals give

$$I_{\pi-\pi'}\propto[\sin(2\theta)\sin(\psi)\cos(\beta)]^2, \tag{A3a}$$

$$I_{\pi-\sigma'}\propto[\cos(\theta)\cos(\psi)\cos(\beta)-\sin(\theta)\sin(\beta)]^2, \tag{A3b}$$

$$I_{\sigma-\sigma'}=0, \tag{A3c}$$

$$I_{\sigma-\pi'}\propto[-\cos(\theta)\cos(\psi)\cos(\beta)-\sin(\theta)\sin(\beta)]^2. \tag{A3d}$$

2. Noncollinear magnetic structure

The Nd moments [see Fig. 5(a)] are divided in Nd moments aligned parallel to the a axis, with $\mathbf{m}_1=(1,0,0)$, and in those aligned along the c axis, with $\mathbf{m}_2=(0,0,1)$. Their (magnetic) structure factors are F_H and F_V, respectively. The Nd magnetic moments are of equal magnitude, $m_1=m_2$. We thus obtain

$$F_H=8(A+iB)f_{\mathrm{Nd}},$$

$$F_V=8(-A+iB)f_{\mathrm{Nd}}, \tag{A4}$$

where A and B are real constants. The total magnetic structure factor equals F_H+F_V. We then obtain for the diffracted intensities

$$I_{\pi-\pi'} \propto \sin(2\theta)\sin(\psi)\{[\sin(\beta)-\cos(\beta)]^2A^2 - [\sin(\beta)-\cos(\beta)]^2B^2\}, \quad \text{(A5a)}$$

$$I_{\pi-\sigma'} \propto A^2\{-\cos(\theta)\cos(\psi)[\cos(\beta)-\sin(\beta)] + \sin(\theta)[\sin(\beta)+\cos(\beta)]\}^2 + B^2\{-\cos(\theta)\cos(\psi)[\cos(\beta)+\sin(\beta)] + \sin(\theta)[\sin(\beta)-\cos(\beta)]\}^2, \quad \text{(A5b)}$$

$$I_{\sigma-\sigma'} = 0, \quad \text{(A5c)}$$

$$I_{\sigma-\pi'} \propto A^2\{\cos(\theta)\cos(\psi)[\cos(\beta)-\sin(\beta)] + \sin(\theta)[\sin(\beta)+\cos(\beta)]\}^2 + B^2\{\cos(\theta)\cos(\psi)[\cos(\beta)+\sin(\beta)] + \sin(\theta)(\sin(\beta)-\cos(\beta))\}^2. \quad \text{(A5d)}$$

The ratio $(I_{\pi-\sigma'}+I_{\pi-\pi'})/(I_{\sigma-\pi'}+I_{\sigma-\sigma'})$ is plotted for both models in Fig. 4.

*scagnoli@esrf.eu

[1] J. L. Garcia-Muñoz, J. Rodriguez-Carvajal, P. Lacorre, and J. B. Torrance, Phys. Rev. B **46**, 4414 (1992).
[2] J. L. Garcia-Muñoz, J. Rodriguez-Carvajal, and P. Lacorre, Europhys. Lett. **20**, 241 (1992).
[3] J. L. Garcia-Muñoz, J. Rodriguez-Carvajal, and P. Lacorre, Phys. Rev. B **50**, 978 (1994).
[4] J. A. Alonso, J. L. Garcia-Muñoz, M. T. Fernandez-Diaz, M. A. G. Aranda, M. J. Martinez-Lope, and M. T. Casais, Phys. Rev. Lett. **82**, 3871 (1999).
[5] U. Staub, G. I. Meijer, F. Fauth, R. Allenspach, J. G. Bednorz, J. Karpinski, S. M. Kazakov, L. Paolasini, and F. d'Acapito, Phys. Rev. Lett. **88**, 126402 (2002).
[6] V. Scagnoli, U. Staub, M. Janousch, A. M. Mulders, M. Shi, G. I. Meijer, S. Rosenkranz, S. B. Wilkins, L. Paolasini, J. Karpinski, S. M. Kazakov, and S. W. Lovesey, Phys. Rev. B **72**, 155111 (2005).
[7] I. I. Mazin, D. I. Khomskii, R. Lengsdorf, J. A. Alonso, W. G. Marshall, R. M. Ibberson, A. Podlesnyak, M. J. Martinez-Lope, and M. M. Abd-Elmeguid, Phys. Rev. Lett. **98**, 176406 (2007).
[8] K. Kuzushita, S. Morimoto, S. Nasu, and S. Nakamura, J. Phys. Soc. Jpn. **69**, 2767 (2000).
[9] M. T. Fernandez-Diaz, J. A. Alonso, M. J. Martinez-Lope, M. T. Casais, and J. L. Garcia-Muñoz, Phys. Rev. B **64**, 144417 (2001).
[10] F. Bartolomé, J. Bartolomé, and R. S. Eccleston, J. Appl. Phys. **87**, 7052 (2000).
[11] V. Scagnoli, U. Staub, A. M. Mulders, M. Janousch, G. I. Meijer, G. Hammerl, J. M. Tonnerre, and N. Stojic, Phys. Rev. B **73**, 100409(R) (2006).
[12] S. W. Cheong and M. Mostovoy, Nat. Mater. **6**, 13 (2007).
[13] D. G. Gibbs, D. R. Harshman, E. D. Isaacs, D. B. McWhan, D. Mills, and C. Vettier, Phys. Rev. Lett. **61**, 1241 (1988).
[14] J. M. Tonnerre, L. Sève, D. Raoux, G. Soullié, B. Rodmacq, and P. Wolfers, Phys. Rev. Lett. **75**, 740 (1995).
[15] S. B. Wilkins, P. D. Hatton, M. D. Roper, D. Prabhakaran, and A. T. Boothroyd, Phys. Rev. Lett. **90**, 187201 (2003).
[16] S. B. Wilkins, P. D. Spencer, P. D. Hatton, S. P. Collins, M. D. Roper, D. Prabhakaran, and A. T. Boothroyd, Phys. Rev. Lett. **91**, 167205 (2003).
[17] S. S. Dhesi, A. Mirone, C. D. Nadai, P. Ohresser, P. Bencok, N. B. Brookes, P. Reutler, A. Revcolevschi, A. Tagliaferri, O. Toulemonde *et al.*, Phys. Rev. Lett. **92**, 056403 (2004).
[18] P. Lacorre, J. B. Torrance, J. Pannetier, A. I. Nazzal, P. W. Wang, and T. C. Huang, J. Solid State Chem. **91**, 225 (1991).
[19] V. Scagnoli, Ph.D. thesis, Swiss Federal Institute of Technology Zurich, 2005.
[20] N. Jaouen, J. M. Tonnerre, G. Kapoujian, P. Taunier, J. P. Roux, D. Raoux, and F. Sirotti, J. Synchrotron Radiat. **11**, 353 (2004).
[21] U. Staub, V. Scagnoli, A. M. Mulders, K. Katsumata, Z. Honda, H. Grimmer, M. Horisberger, and J. M. Tonnerre, Phys. Rev. B **71**, 214421 (2005).
[22] D. B. McWhan, C. Vettier, E. D. Isaacs, G. E. Ice, D. P. Siddons, J. B. Hastings, C. Peters, and O. Vogt, Phys. Rev. B **42**, 6007 (1990).
[23] J. P. Hannon, G. T. Trammell, M. Blume, and D. Gibbs, Phys. Rev. Lett. **61**, 1245 (1988).
[24] D. Templeton and L. Templeton, Acta Crystallogr., Sect. A: Cryst. Phys., Diffr., Theor. Gen. Crystallogr. **36**, 237 (1980).
[25] S. W. Lovesey, E. Balcar, K. S. Knight, and J. F. Rodriguez, Phys. Rep. **411**, 233 (2005).
[26] N. W. Ashcroft and N. D. Mermin, *Solid State Physics* (Saunders College Publishing, Philadelphia, PA, 1976).
[27] J. P. Hill, A. Vigliante, D. Gibbs, J. L. Peng, and R. L. Greene, Phys. Rev. B **52**, 6575 (1995).
[28] J. P. Hill and D. F. McMorrow, Acta Crystallogr., Sect. A: Found. Crystallogr. **52**, 236 (1996).